Journal of Fluorescence, Vol. 16, No. 3, May 2006 (© 2006)
DOI: 10.1007/s10895-005-0065-5

Regionalization of Plasma Membrane-Bound Flavoproteins of Cerebellar Granule Neurons in Culture by Fluorescence Energy Transfer Imaging

Alejandro K. Samhan-Arias,[1] Miguel A. García-Bereguiaín,[1] Francisco Javier Martín-Romero,[1] and Carlos Gutiérrez-Merino [1,2]

Received November 1, 2005; accepted December 29, 2005
Published online: March 15, 2006

Flavoproteins are components of plasma membrane redox chains, which have been suggested to play major roles in neuronal activity and survival. We found that the red/orange autofluorescence of mature primary cultures of cerebellar granule neurons (8–9 days in vitro) was largely quenched by millimolar concentrations of dithionite added to the extracellular medium, and pointed out that nearly 50% of this autofluorescence was due to plasma membrane-bound flavoproteins. We report in this work that the lipophilic neuronal plasma membrane markers *N*-(3-triethylammoniumpropyl)-4-(4-(4-(diethylamino)phenyl)butadienyl)-pyridinium dibromide (RH-414) and *N*-(3-triethylammoniumpropyl)-4-(6-(4-(diethylamino)phenyl)hexatrienyl)pyridinium dibromide (FM4-64) can form fluorescence energy transfer donor–acceptor pairs with flavoproteins with calculated R_0 values between 3.7 and 4.2 nm. The quantification of the efficiency of fluorescence energy transfer with different concentrations of acceptor dyes has been worked out with re-suspended neurons. Using quantitative images of the neurons in culture, acquired with a CCD camera attached to an epifluorescence microscope, regionalization of the plasma membrane-bound flavoproteins of cerebellar granule neurons has been achieved from the quenching by dithionite of the fluorescence of the acceptor dye. The results unraveled that plasma membrane-bound flavoproteins are largely enriched in interneuronal contact sites forming clusters of 0.5–1 μm diameter size, which appears largely regionalized in the neuron's cell body.

KEY WORDS: Flavoproteins; Fluorescence energy transfer; Imaging; Neurons; Plasma membrane.

INTRODUCTION

The presence of a plasma membrane redox chain in several mammalian cell lines has been reported during last 20 years [1,2], and also to be widely present in different brain regions [3]. Activation of transplasma membrane oxidoreductase is related to exocytosis of chlatrin-coated vesicles as well as to receptor-mediated and adsorptive endocytosis [4]. The plasma membrane redox chain plays a major role in ascorbate free radical recycling [2,3] and superoxide anion production at the external surface of neurons [5], and its deregulation is a critical event at the onset of cerebellar granule neurons apoptosis induced by lowering potassium in the culture medium [6]. The flavoprotein cytochrome b_5 reductase has been shown to be a major component of the mammalian plasma membrane redox chain [7,8], and other flavoproteins with NAD(P)H oxidase activity had been shown to be bound to the mammalian plasma membrane, for example in glial cells and in macrophages [9,10]. Changes of the red/orange autofluorescence of embryonic brain neurons have been reported under cellular oxidative stress conditions [11].

[1] Departamento de Bioquímica y Biología Molecular y Genética, Facultad de Ciencias, Universidad de Extremadura, Avda. de Elvas, s/n., 06071, Badajoz, Spain.
[2] To whom correspondence should be addressed. E-mail: carlosgm@unex.es.

Fluorescence resonance energy transfer (FRET) has been shown to be a valuable tool to address topological issues in membrane proteins, see, e.g., previous works from our laboratory [12–14]. In particular, FRET from fluorescent flavoproteins to plasma membrane lipid acceptors is an unexplored issue in neurons up to date. This is a particular case of FRET from one donor to multiple acceptors in a two-dimensional lipid bilayer array, for which the basic formalism was worked in [15,16], and later applied to reconstituted membrane proteins, like the sarcoplasmic reticulum Ca^{2+}-ATPase [12] and the nicotinic receptor [14]. The sum of the FRET between donor and each of the putative acceptors allows to have a significant FRET efficiency with very low lipid molar fractions of acceptors (usually less than 1%), and as a side advantage the theoretical orientation factor approaches to 2/3 for randomly-distributed lipid acceptors. A major methodological conclusion from these studies was that only a limited number of lipid shells around the donor-containing protein significantly contributed to FRET for an acceptor lipid randomly distributed in the lipid bilayer [12,16,17]. This implied that FRET extends only several nanometers away from the position of the donor protein, which is particularly useful for spatial resolution in cell imaging.

During last years several lipophilic plasma membrane dyes have been developed and tested in neurons in culture. Two of these dyes, *N*-(3-triethylammoniumpropyl)-4-(4-(4-(diethylamino)phenyl) butadienyl)-pyridinium dibromide (RH-414) and *N*-(3-triethylammoniumpropyl)-4-(6-(4-(diethylamino)phenyl)hexatrienyl)pyridinium dibromide (FM4-64) have spectral characteristics that make them candidates of choice as putative acceptors of the fluorescence emission of flavins, as the fluorescence of flavins (peak emission between 520 and 530 nm) is close to their maximum absorption wavelengths (520–525 nm for FM4-64 bound to zwitterionic CHAPS micelles and 532 nm for RH-414 in DMSO) and they have a large extinction coefficient [18]. The fluorescence of RH-414 has been shown to be homogeneously distributed in the plasma membrane of several neurons in culture, evenly staining the cell body and the neurite extensions [18,19], whereas that of FM4-64 stains more specifically active membrane recycling at synaptic connections [20].

In this paper, we show the regional compartmentation of the plasma membrane flavoproteins fluorescence (red/orange autofluorescence sensitive to dithionite) using fluorescence energy transfer to plasma membrane dye markers. Our results show that the plasma membrane-bound flavoproteins fluorescence accounts for 30–40% of the total red/orange autofluorescence of cerebellar granule cells, forming clusters of 0.5–1 μm diameter which are largely enriched in interneuronal contact sites.

MATERIALS AND METHODS

Cerebellar Granule Cells Primary Cultures

Cultures of cerebellar granule neurons (CGN) were obtained from dissociated cerebella of 7-days-old Wistar rats as described previously [6,21]. Cells were plated in Dulbecco's modified Eagle's medium (DMEM) supplemented with 10% heat-inactivated fetal bovine serum, 0.1 mg/mL gentamicin and 25 mM KCl on 35-mm dishes coated with poly-D-lysine, at a density of 2.5×10^6 cells/dish. Cultures were maintained at 37°C in a humidified atmosphere of 95% air/5% CO_2. Cytosine arabinofuranoside (10 μM) was added to fresh culture medium 48 h after plating to prevent replication of non-neuronal cells. All experiments were performed using mature CGN at 8–9 days, in vitro. The culture medium was replaced with Locke's K25 buffer 15–20 min before fluorescence measurements, or acquisition of fluorescence microscopy images.

The composition of the Locke's K25 buffer (pH 7.4 at 37°C) used throughout this work is as follows: 4 mM $NaHCO_3$, 10 mM HEPES, 5 mM glucose, 2.3 mM $CaCl_2$, 1 mM $MgCl_2$, and 134 mM NaCl/25 mM KCl.

The phospholipid content per plate was determined as total phosphorous after perchloric digestion, using ammonium molibdate and ascorbate [22]. Using an average molecular weight of 750 per phospholipid, it was found to be 100–120 nmoles per plate, thus, the phospholipid concentration was 50–60 μM when the cells are re-suspended in 2 mL Locke's K25 buffer.

Fluorescence Measurements

Fluorescence measurements have been carried out with Perkin-Elmer, mod. 650-40 operated in ratio mode, and with SLM-4800C fluorescence spectrophotometers, both equipped with thermostatic cell holders. SLM-4800C was used for measurements of the corrected emission spectra.

Inner filter corrections due to the absorbance of FM4-64 and RH-414 at the excitation and emission wavelengths of flavins fluorescence, 460 and 520 nm, respectively, were done as indicated in [23], using the experimentally determined extinction coefficients for FM4-64 and RH-414 in dimethyl sulfoxide. The values obtained for the extinction coefficients were: $\varepsilon_{460nm} = 19{,}500\ M^{-1}\ cm^{-1}$ and $\varepsilon_{520nm} = 46{,}200\ M^{-1}\ cm^{-1}$ for FM4-64

and $\varepsilon_{460nm} = 24{,}000\ M^{-1}\ cm^{-1}$ and $\varepsilon_{520nm} = 53{,}530\ M^{-1}\ cm^{-1}$ for RH-414. Thus, the inner filter fluorescence correction was lower than 5% up to 0.6 μM FM4-64 and up to 0.54 μM RH-414.

Calculation of the FRET Donor–Acceptor Pair Parameters J and R_0

The FRET donor–acceptor pair parameters J (spectra overlap integral) and R_0 (distance for 50% FRET efficiency) were calculated as indicated for another donor–acceptor pairs in previous papers from this laboratory [12,13,24]. For the case of R_0 values calculations the refractive index was set equal to that of a dilute aqueous solution (1.33) and K^2 (the orientation factor) = 2/3. As the quantum yield of the plasma membrane-bound flavoproteins in CGN is not known we have used a range of quantum yield values of (0.05–0.1) on the basis of those reported for isolated flavoproteins closely related to cytochrome b_5 reductase, like cytochrome P450 reductase [25].

Fluorescence Microscopy Imaging

Digital and quantitative fluorescence images were acquired with a Hamamatsu Hisca CCD camera, attached to a Nikon Diaphot 300 microscope, equipped with a thermostatic plate holder set at 37°C. The camera was set at the highest resolution (2 × 2 binning mode) for all the images shown in this paper. The excitation filters, dichroic mirrors and barrier emission filters used are given in the legends for the Figures. To minimize photobleaching effects on CGN fluorescence, the camera gain and time of exposure was fixed with a separate CGN plate that was discarded (not used for quantitative measurements). The phase contrast masks were obtained after acquisition of the fluorescence images for the same field of the plate, keeping constant the camera gain and time of exposure with weak illumination with the microscope lamp and without irradiation with the fluorescence lamp (all the slits of the epifluorescence accessory closed). The overall intensity signal of the selected areas of observation were obtained with the Hamamatsu Hisca CCD software.

Chemicals

DMEM, heat inactivated fetal bovine serum, apotransferrin, insulin, progesterone, gentamicin, penicillin, streptomycin, pyruvate, glutamine, cytosine arabinofuranoside, poly-D-lysine and sodium dithionite were obtained from Sigma. FM4-64 and RH-414 were obtained from Molecular Probes. All other chemicals were of the highest quality available, and supplied by Sigma or Roche Molecular Biochemicals.

Sodium dithionite was prepared immediately before use at a concentration of 70 mM in 10 mg/mL sodium bicarbonate solution, kept on ice and used for at most

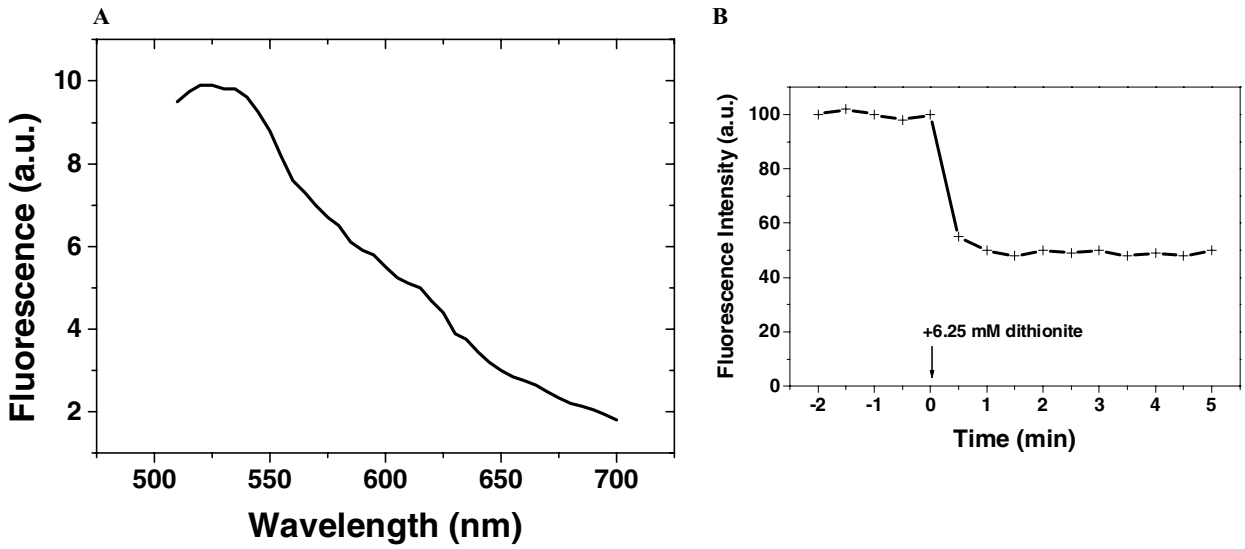

Fig. 1. Red/orange autofluorescence of CGN. CGN at 9 days in vitro were gently scrapped from the plate and re-suspended in 2 mL Locke's K25 buffer. (*Panel A*) Fluorescence emission spectra of re-suspended CGN. (*Panel B*) Sodium dithionite added to the extracellular medium rapidly quenched nearly 50% of the fluorescence at 542 nm (excitation wavelength 460 nm) of re-suspended CGN. The results shown are the average of experiments done with three different CGN preparation, in each case by duplicate (2 plates per preparation, $n = 6$).

30 min. The pH of the Locke's K25 buffer changed less than 0.1 pH units after addition of up to 200 μL of the stock dithionite solution in 2 mL Locke's K25 buffer (final dithionite concentration of 6.25 mM).

RESULTS AND DISCUSSION

Red/orange Autofluorescence of Mature CGN is Largely Flavins Fluorescence

Flavins fluorescence have a characteristic excitation peak centered at 450–460 nm [23]. The emission spectra (excitation wavelength = 460 nm) of CGN resuspended in Locke's K25 buffered solution is shown in the Fig. 1A. This spectrum is consistent with a large contribution of flavins fluorescence to the red/orange autofluorescence of CGN, because the peak emission wavelength closely fit within those of FMN and FAD ([26] and *results not shown*). To further assess this point, we performed a titration of CGN autofluorescence with dithionite, a well established and potent reductant of flavins, which leads to a large quenching of their fluorescence [26]. Figure 1B shows that addition of dithionite to the extracellular Locke's K25 medium promoted (50 ± 3)% decrease of the red/orange autofluorescence of re-suspended CGN in less than 1 min. Moreover, the quenching of CGN fluorescence by dithionite was found to take place at a concentration identical to that found to produce (98–99)% quenching of the fluorescence of FMN and FAD (Fig. 2).

As dithionite is not permeable through the plasma membrane of mammalian cells [27], this result suggested that a large fraction of flavins fluorescence of CGN was due to plasma membrane-bound flavoproteins. This point was experimentally assessed in our re-suspended CGN, since after plasma membrane solubilization with the addition of 0.1% TX-100 the quenching by dithionite rise to (87 ± 3)% of the total CGN autofluorescence. Thus, we considered the possibility of using neuronal plasma membrane dye markers as acceptors for the fluorescence of this pool of CGN flavoproteins, aiming on the one hand to confirm the presence of a large fraction of total flavoproteins as plasma membrane-bound flavoproteins, and on the other hand to regionalize their distribution within the major morphological regions of CGN (i.e., cell body and neurites).

Neuronal Plasma Dye Markers FM4-64 and RH-414 can be Used as Acceptors of Membrane-Bound Flavins Fluorescence of CGN in Culture

The absorption and fluorescence emission spectra of the neuronal plasma membrane dyes FM4-64 and RH-414 were recorded 15–30 min after mixing with

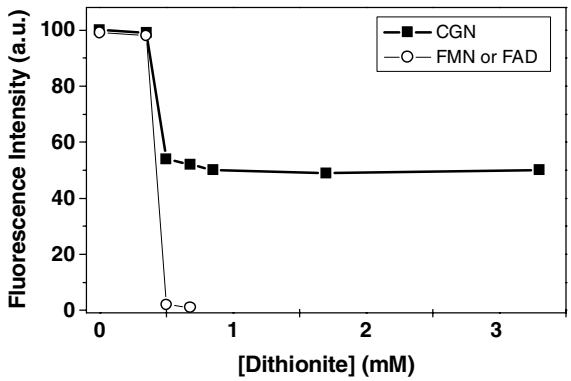

Fig. 2. Titration with extracellular dithionite of the red/orange autofluorescence of CGN. CGN were gently scrapped from the plate and re-suspended in 2 mL of Locke's K25 buffer. Solid squares: re-suspended CGN, and open circles: 10 μM FMN or FAD in Locke's K25 buffer. The fluorescence of the control samples (before addition of dithionite) was normalized to 100% to allow for a direct comparison between CGN and FMN or FAD fluorescence quenching by dithionite, and the data points of the fluorescence of FMN and FAD for dithionite concentrations lower than 0.5 mM has been slightly shifted by -(1–2%) to avoid complete overlap between solid squares and open circles. The fluorescence of FMN and FAD were more than 98% quenched by $\geq$ 0.7 mM dithionite. For all the cases the excitation wavelength was set at 460 nm and the emission wavelengths were set close to the experimentally determined emission peak wavelengths for each sample, namely, 542 nm for CGN, and 525 nm for FMN and FAD.

50 μM egg lecithin liposomes in Locke's K25 buffer (*results not shown*). This concentration of egg lecithin liposomes was used because it is close to the total lipid concentration determined in our culture plates containing 2.5 millions of CGN (see Section ''Materials and Methods''). Thereafter, the overlap integral with the emission spectra of re-suspended CGN was calculated as indicated in Section ''Materials and Methods'' and the values of the distance range for 50% fluorescence energy transfer efficiency, R_0, was obtained for the range of quantum yields reported for several standard flavoproteins (Table I). Thus, the results showed that both FM4-64 and RH-414 can be used as efficient acceptors of the red/orange autofluorescence of plasma membrane-bound flavins of CGN. In addition, the dependence of the fluorescence intensity of both FM4-64 and RH-414 incorporated into egg lecithin liposomes is linear with the dye concentration within the submicromolar concentration range (Fig. 3A), thus, excluding significant quenching effects due to photon migration within acceptors in this concentration range.

Since a weak FM4-64 and RH-414 fluorescence emission can be detected with excitation at 460 nm (the flavins excitation wavelength), the possibility of direct effects of dithionite on the fluorescence emission of these dyes deserved to be studied, as dithionite will be used

Table I. FRET Parameters for FM4-64 and RH-414 as Acceptors of the Flavin Fluorescence of Cytochrome P450 Reductase-like CGN Flavoproteins

Donor/acceptor pair	J (cm^3 M^{-1})	Q_D[a]	n	K^2	R_0 (nm)
Flavoprotein/FM4-64	3.105×10^{-13}	0.05	1.33	2/3	3.8
	3.105×10^{-13}	0.1	1.33	2/3	4.2
Flavoprotein/RH-414	2.8×10^{-13}	0.05	1.33	2/3	3.7
	2.8×10^{-13}	0.1	1.33	2/3	4.15

[a] $Q_D = 0.063$ for cytochrome P450 reductase [25].

to quantify the contribution of flavins through FRET to the acceptor dye in CGN. The results obtained are shown in the Fig. 3B and pointed out that RH-414 is partially quenched by dithionite (11 and 26% by 1.7 and 3.3 mM dithionite, respectively) whereas FM4-64 fluorescence is not significantly quenched (less than 5% quenching) by dithionite concentrations affording (98–99)% quenching of the fluorescence of FMN or FAD. Therefore, FM4-64 is superior to RH-414 as acceptor dye for FRET imaging of plasma membrane-bound flavoproteins in CGN, and it was selected for the experiments with dithionite done in the rest of this study.

FRET from Plasma Membrane-Bound Flavoproteins to FM4-64 from Fluorescence Microscopy Images

The fluorescence at 520 nm (excitation wavelength 460 nm) of re-suspended CGN was $32 \pm 5\%$ quenched by incorporation of FM4-64 or RH-414 to the plasma membrane due to FRET (Fig. 4A). In this regard, RH-414 is a cleaner acceptor dye because it has not any significant fluorescence emission at this wavelength with excitation at 460 nm, whereas correction for the weak fluorescence of FM4-64 at 520 nm was needed (Fig. 4B). In this latter case, correction was done taking advantage of the very different ratios of the red/orange autofluorescence and that of FM4-64 at 670 and 520 nm (compare Fig. 1A and 4B). The results shown in the Fig. 4 indicated that 0.2 μM FM4-64 is the concentration producing nearly half-saturation FRET efficiency, and we decided to avoid higher concentration of FM4-64 to minimize: (i) the occurrence of photon migration between acceptors, and (ii) the incorporation of FM4-64 to membranes of subcellular organelles. Also to minimize this latter possibility the measurements were taken shortly after addition of FM4-64, between 5 and 10 min. A collateral advantage of the use of 0.2 μM FM4-64 is that the intensity of fluorescence on the acceptor side was nearly the same as the intensity of fluorescence on the donor side before the injection

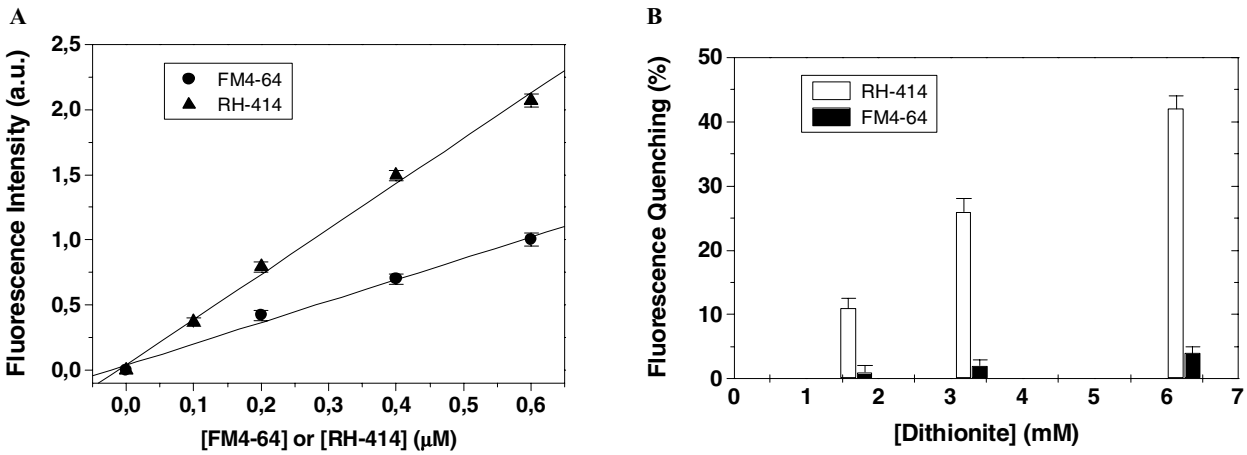

Fig. 3. Fluorescence of FM4-64 and RH-414 incorporated in egg lecithin liposomes. (*Panel A*) Linearity up to 0.6 μM of the fluorescence intensity of FM4-64 (solid circles; excitation 460 nm and emission 650 nm) and RH-414 (up-triangles; excitation 460 nm and emission 670 nm) incorporated in 50 μM egg lecithin liposomes. (*Panel B*) Quenching by dithionite of the fluorescence of FM4-64 (black bars) and of RH-414 (white bars) incorporated in egg lecithin liposomes. FM4-64 and RH-414 concentration was 0.5 μM and incubated for at least 15 min with egg lecithin liposomes before fluorescence measurements and after dithionite addition fluorescence readings were taken during 5–10 min. All the results shown are the average of experiments done by triplicate.

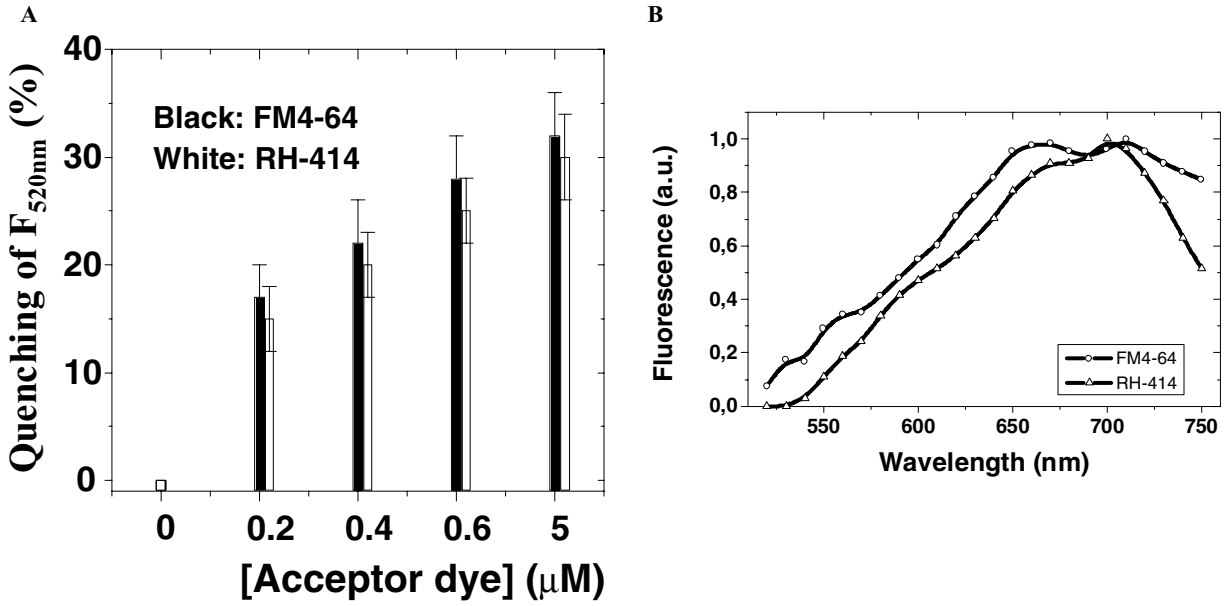

Fig. 4. Quenching of CGN's flavins fluorescence by FRET to the plasma membrane lipid markers FM4-64 and RH-414. FM4-64 and RH-414 were added from a concentrated stock solution in DMSO to CGN re-suspended in Locke's K25 buffer, and incubated for 15 min, before recording the fluorescence emission spectra (a time sufficient for complete incorporation of the dyes to CGN, as assessed with fluorescence microscopy images). (*Panel A*) The quenching of the fluorescence of CGN flavins was monitored at 520 nm (excitation 460 nm) to minimize the contribution of the fluorescence of the acceptor dyes. Black bars: FM4-64; white bars: RH-414. Inner filter corrections were done when appropriate as indicated in Section ''Materials and Methods.'' Similar results were obtained from the overall green fluorescence of non-detached CGN in microscopy images acquired with the Hamamatsu Hisca CCD camera using an excitation filter of 470 nm, dichroic mirror of 510 nm and barrier emission filter of 520 nm. (*Panel B*) Normalized emission spectra of FM4-64 (and RH-414 incorporated in egg lecithin liposomes. The contribution of the scattering of the 50 μM egg lecithin liposomes was subtracted, and the spectra shown in the Figure are the average of spectra recorded with concentrations of FM4-64 and RH-414 ranging from 0.5 to 2 μM. The buffer used for all these measurements was Locke's K25.

of FM4-64 to CGN. As a consequence FRET will be expected to produce an increase of the fluorescence of the acceptor close to the fluorescence quenching observed for the donor.

The observation of CGN under the fluorescence microscope after supplementation with 0.2 μM FM4-64 reveals a ring-like pattern for neurons that are not forming granules or neurons nests (Fig. 5), pointing out a large contribution of the plasma membrane to the fluorescence image. To better visualize this point the fluorescence image was mounted over a phase contrast mask of the same field of neurons, acquired with the Hamamatsu Hisca CCD camera. The overall brightness in all the pixels of the frame of the phase contrast mask was 15% of the total fluorescence intensity for the image shown in the Fig. 5. The images shown in the Fig. 5 are representative of those obtained with three different CGN preparations, and $n > 500$ cell bodies. Addition of dithionite produced a large quenching of the fluorescence image, particularly in the external ring of the neuron's cell body (Fig. 5C). The quenching was already seen for the very first image taken routinely 1–2 min after dithionite addition, and was sustained for at least 10–15 min. The overall quenching by dithionite of the fluorescence of FM4-64 incorporated into CGN was quantified from the accumulated intensity of all the pixels of the acquired image, read with the Hamamatsu Hisca CCD software, and was found to be $25 \pm 3\%$ ($n = 10$ frames of different plates corresponding to three different CGN preparations). This result is in excellent agreement with the quenching of the red/orange autofluorescence of re-suspended CGN by 0.2 μM FM4-64 (Fig. 4), and allows to conclude that this was due to FRET between plasma membrane-bound flavoproteins and FM4-64.

To further highlight the localization of flavoproteins acting as donor for FRET to FM4-64 we have obtained the quantitative difference image between the images shown in Fig. 5B (before addition of dithionite) and Fig. 5C (after addition of dithionite). To this end, the quantitative images acquired with the Hamamatsu Hisca CCD were exported in black and white. To subtract the image after addition of dithionite, this image was inverted.

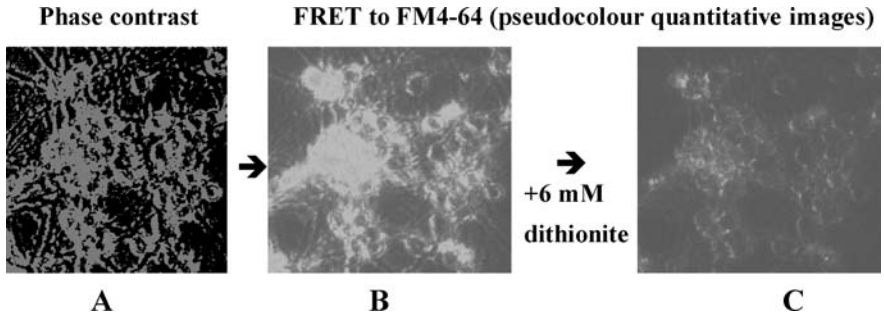

Fig. 5. Fluorescence microscopy images of CGN stained with FM4-64 highlight that the quenching of flavins fluorescence by dithionite takes place largely at the neurons plasma membrane. The plasma membrane lipophilic fluorescent marker FM4-64 has been used as acceptor for the red/orange fluorescence emission of plasma membrane-bound flavins. As the fluorescence of FM4-64 is not sensitive to dithionite, the strong quenching of the fluorescence of FM4-64 incorporated into CGN demonstrated a large contribution of FRET from plasma membrane-bound flavins to FM4-64 fluorescence emission. Aiming to a better visual localization of fluorescence in CGN the fluorescence color-coded images were mounted onto a phase contrast mask, shown in the left image (*Panel A*), which accounts for 15% of the total fluorescence intensity signal of the image shown in *Panel B*. Representative images of the same group of CGN (9 days in vitro) in Locke's K25 medium plus 0.2 (M FM4-64 before and after the addition of 6 mM dithionite, *Panels B and C*, respectively. The images were obtained with a Hamamatsu Hisca CCD camera attached to an epifluorescence Nikon Diaphot 300 microscope, using a 470 nm excitation filter plus a 580 nm dichroic mirror and 590nm barrier emission filter (exposure time: 205.7 ms for CGN + FM4-64).

The difference image shown in the Fig. 6 is the result of superimposing the image obtained before addition of dithionite on the inverted image after addition of dithionite, each with 50% transparency. This image (which is representative of many other similar images) showed that FRET between plasma membrane-bound flavoproteins and FM4-64 is clustered to patches or discrete membrane domains, and is not homogeneously dispersed within the neuronal plasma membrane. The possibility that this is merely reflecting a non-homogeneous distribution of the acceptor FM4-64 in the CGN plasma membrane can be excluded, on the basis of the more diffuse distribution of FM4-64 fluorescence when excited at 510 nm (*results not shown*). However, it is to be noted that for FRET between donors located on an integral membrane protein and lipid acceptors the maximum FRET efficiency at high density of lipid acceptors is dependent on the lipid acceptor partition between the two-leaflets of the lipid bilayer and on the extent of binding of the acceptor (FM4-64 in this case) to the annular lipids binding domains of plasma membrane-bound donors (flavoproteins), e.g., FM4-64 exclusion from or preferential partition in the lipids annulus, as shown in [14,16,17,28]. As FRET from a donor located in a membrane-bound protein to an acceptor in the lipid bilayer vanishes rapidly after only several lipid shells around the protein, i.e., only in several nm [12,16], the occurrence of membrane domains of 0.5–1 μm diameter like those seen in the Fig. 6 indicated the occurrence of clusters of plasma membrane-bound flavoproteins in the CGN in culture. This result is fully consistent with the reported functional link between the activation of transplasma membrane oxidoreductase and exocytosis of chlatrin-coated vesicles [4]. Furthermore, the results pointed out that plasma membrane-bound flavoproteins are regionalized in the neurons cell body and highly enriched in interneuronal contact sites within the granules.

CONCLUSIONS

1. FM4-64 and RH-414 can act as acceptors for the fluorescence of plasma membrane-bound flavoproteins with R_0 values in the range of 3.7–4.2 nm.
2. Both, the quenching of the CGN red/orange autofluorescence by dithionite a short time after its addition to the culture medium and the quenching by the plasma membrane lipid markers FM4-64 and RH-414 point out that the plasma membrane-bound flavins accounts for nearly half of total red/orange fluorescence of CGN.
3. FRET efficiency from CGN's flavins to lipid acceptors in the plasma membrane reaches (30–35)% in mature CGN at 9 days in vitro.

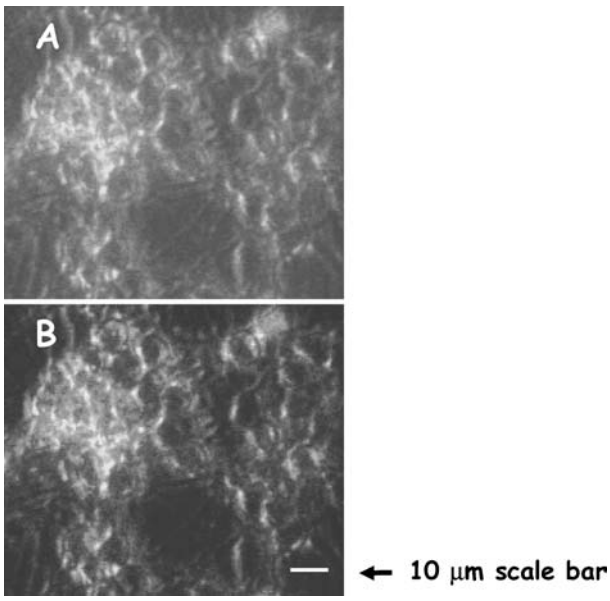

Fig. 6. Regionalization of plasma membrane CGN's red/orange flavins fluorescence using FRET to FM4-64. Difference image of CGN obtained from the same field of neurons before and after addition of dithionite (mounted onto a phase contrast mask accounting for 15% of the fluorescence signal intensity for a better visual localization). (*Panel A*) Black and white image. (*Panel B*) The fluorescence intensity is shown in magenta with the highest intensity spots in white, and the phase contrast mask is shown in blue.

4. The plasma membrane flavins fluorescence in CGN is largely compartmented in interneuronal contact sites forming clusters of 0.5–1 μm diameter size, which appears largely regionalized in the neuron's cell body.

ACKNOWLEDGMENTS

This work has been supported by Grant SAF2003-08275 of the Spanish Ministerio de Ciencia y Tecnología. AKSA and MAGB are recipient of predoctoral fellowships of the Junta de Extremadura and Spanish Ministerio de Ciencia y Tecnología, respectively.

REFERENCES

1. F. L. Crane, H. Löw, and M. G. Clark (1985). Transplasma-membrane redox system in growth and development. *Biochim. Biophys. Acta* **811**(3), 233–266.
2. J. M. May (1999). Is ascorbic acid an antioxidant for the plasma membrane? *FASEB J.* **13**(9), 995–1006.
3. Y. Yong and J. L. Dreyer (1995). Distribution of six transplasma membrane NADH-dehydrogenases in rat brain tissue. *Brain Res. Dev. Brain Res.* **89**(2), 235–252.
4. J. L. Dreyer (1990). Plasma membrane dehydrogenases in rat brain synaptic membranes. Multiplicity and subunit composition. *J. Bioenerg. Biomembr.* **22**(5), 619–633.
5. F. J. Martin-Romero, Y. Gutierrez-Martin, F. Henao, and C. Gutierrez-Merino (2002). The NADH oxidase activity of the plasma membrane of synaptosomes is a major source of superoxide anion and is inhibited by peroxynitrite. *J. Neurochem.* **82**(3), 604–614.
6. F. J. Martin-Romero, E. Garcia-Martin, and C. Gutierrez-Merino (2002). Inhibition of oxidative stress produced by plasma membrane NADH oxidase delays low-potassium-induced apoptosis of cerebellar granule cells. *J. Neurochem.* **82**(3), 705–715.
7. J. M. Villalba, F. Navarro, F. Cordoba, A. Serrano, A. Arroyo, F. L. Crane, and P. Navas (1995). Coenzyme Q reductase from liver plasma membrane: purification and role in trans-plasma-membrane electron transport. *Proc. Natl. Acad. Sci. USA* **92**(11), 4887–4891.
8. C. Kim, F. L. Crane, W. P. Faulk, and D. J. Morre (2002). Purification and characterization of a doxorubicin-inhibited NADH-quinone (NADH-ferricyanide) reductase from rat liver plasma membranes. *J. Biol. Chem.* **277**(19), 16441–16447.
9. A. Kindzelskii and H. R. Petty (2004). Fluorescence spectroscopic detection of mitochondrial flavoprotein redox oscillations and transient reduction of the NADPH oxidase-associated flavoprotein in leukocytes. *Eur. Biophys. J.* **33**(4), 291–299.
10. J. E. Brenman and D. S. Bredt (1997). Synaptic signaling by nitric oxide. *Curr. Opin. Neurobiol.* **7**(3), 374–378.
11. L. Eide, and C. T. McMurray (2005). Culture of adult mouse neurons. *BioTechniques* **38**(1), 99–104.
12. C. Gutiérrez-Merino, F. Munkonge, A. M. Mata, J. M. East, B. L. Levinson, R. M. Napier, and A. G. Lee (1987). The position of the ATP binding site on the (Ca^{2+}, + Mg^{2+})-ATPase. *Biochim. Biophys. Acta* **897**(2), 207–216.
13. F. Centeno, and C. Gutiérrez-Merino (1992). Location of functional centers in the microsomal cytochrome P450 system. *Biochemistry* **31**(36), 8473–8481.
14. C. Gutiérrez-Merino, I. C. Bonini de Romanelli, L. I. Pietrasanta, and F. J. Barrantes (1995). Preferential distribution of the fluorescent phospholipid probes NBD-phosphatidylcholine and rhodamine-phosphatidylethanolamine in the exofacial leaflet of acetylcholine receptor-rich membranes from *Torpedo marmorata*. *Biochemistry* **34**(14), 4846–4855.
15. C. Gutiérrez-Merino (1981). Quantitation of the Forster energy transfer for two-dimensional systems. I. Lateral phase separation in unilamellar vesicles formed by binary phospholipid mixtures. *Biophys. Chem.* **14**(3), 247–257.
16. C. Gutiérrez-Merino (1981). Quantitation of the Forster energy transfer for two-dimensional systems. II. Protein distribution and aggregation state in biological membranes. *Biophys. Chem.* **14**(3), 259–266.
17. C. Gutiérrez-Merino, F. Centeno, E. Garcia-Martin, and J. M. Merino (1994). Fluorescence energy transfer as a tool to locate functional sites in membrane proteins. *Biochem. Soc. Trans.* **22**(3), 784–788.
18. R. P. Haugland (2005). *The Handbook: A Guide to Fluorescent Probes and Labeling Techniques*, 10th ed., (editor Michelle T.Z. Spence), pages 585,587,676,788-989 and 976-978. Molecular Probes/Invitrogen, Carlsbad(California, USA).
19. D. Schild, H. Geiling, and J. Bischofberger (1995). Imaging of L-type Ca^{2+} channels in olfactory bulb neurones using fluorescent dihydropyridine and a styryl dye. *J. Neurosci. Methods* **59**(2), 183–190.
20. R. A. McKinney (2005). Physiological roles of spine motility: development plasticity and disorders. *Biochem. Soc. Trans.* **33**(6), 1299–1302.
21. A. K. Samhan-Arias, F. J. Martin-Romero, and C. Gutierrez-Merino (2004). Kaempferol blocks oxidative stress in cerebellar granule cells and reveals a key role for reactive oxygen species production at the plasma membrane in the commitment to apoptosis. *Free Radic. Biol. Med.* **37**(1), 48–61.

22. R. Letters (1964). The application of a two-dimensional paper-chromatographic technique to the analysis of phospholipids. *Biochem. J.* **93**, 313–316.
23. J. R. Lakowicz (1999). *Principles of Fluorescence Spectroscopy* 2nd ed, Kluwer Academic/Plenum Press, New York.
24. C. Gutiérrez-Merino, A. Molina, B. Escudero, A. Diez, and J. Laynez (1989). Interaction of the local anesthetics dibucaine and tetracaine with sarcoplasmic reticulum membranes. Differential scanning calorimetry and fluorescence studies. *Biochemistry* **28**(8), 3398–3406.
25. P. I. Bastiaens, P. J. Bonants, F. Muller, and A. J. Visser (1989). Time-resolved fluorescence spectroscopy of NADPH-cytochromeP-450 reductase: demonstration of energy transfer between the two prosthetic groups. *Biochemistry* **28**(21), 8416–8425.
26. J. Koziol (1971). Fluorometric analyses of riboflavin and its coenzymes. *Methods Enzymol* **XVIII** (Part B), 253–285.
27. W. H. Lawson, Jr., R. A. Holland, and R. E. Forster (1965). Effect of temperature on deoxygenation rate of human red cells. *J. Appl. Physiol.* **20**(5), 912–918.
28. S. S. Antollini, M. A. Soto, I. Bonini de Romanelli, C. Gutiérrez-Merino, P. Sotomayor, and F. J. Barrantes (1996). Physical state of bulk and protein-associated lipid in nicotinic acetylcholine receptor-rich membrane studied by laurdan generalized polarization and fluorescence energy transfer. *Biophys. J.* **70**(3), 1275–1284.